HHS Public Access

Author manuscript

Nat Biomed Eng. Author manuscript; available in PMC 2017 October 04.

Published in final edited form as:

Nat Biomed Eng. 2016 ; 1: . doi:10.1038/s41551-016-0002.

A brush-polymer conjugate of exendin-4 reduces blood glucose for up to five days and eliminates poly(ethylene glycol) antigenicity

Yizhi Qi[1], **Antonina Simakova**[2], **Nancy J. Ganson**[3], **Xinghai Li**[1], **Kelli M. Luginbuhl**[1], **Imran Özer**[1], **Wenge Liu**[1], **Michael S. Hershfield**[3,4], **Krzysztof Matyjaszewski**[2], and **Ashutosh Chilkoti**[1,*]

[1]Department of Biomedical Engineering, Duke University, Durham, NC, USA

[2]Department of Chemistry, Carnegie Mellon University, Pittsburgh, PA, USA

[3]Department of Medicine, Division of Rheumatology, Duke University Medical Center, Durham, NC, USA

[4]Department of Biochemistry, Duke University School of Medicine, Durham, NC, USA

Abstract

The delivery of therapeutic peptides and proteins is often challenged by a short half-life, and thus the need for frequent injections that limit efficacy, reduce patient compliance and increase treatment cost. Here, we demonstrate that a single subcutaneous injection of site-specific (C-terminal) conjugates of exendin-4 (exendin) — a therapeutic peptide that is clinically used to treat type 2 diabetes — and poly[oligo(ethylene glycol) methyl ether methacrylate] (POEGMA) with precisely controlled molecular weights lowered blood glucose for up to 120 h in fed mice. Most notably, we show that an exendin-C-POEGMA conjugate with an average of 9 side-chain ethylene glycol (EG) repeats exhibits significantly lower reactivity towards patient-derived anti-poly(ethylene glycol) (PEG) antibodies than two FDA-approved PEGylated drugs, and that reducing the side-chain length to 3 EG repeats completely eliminates PEG antigenicity without compromising *in vivo* efficacy. Our findings establish the site-specific conjugation of POEGMA as a next-generation PEGylation technology for improving the pharmacological performance of

*To whom correspondence should be addressed: chilkoti@duke.edu.

Author Contributions

Y.Q. and A.C. conceived and designed the research; Y.Q., A.S., N.J.G., X.L, I.Ö. and W.L. performed the experiments; A.S. and K.M. provided technical expertise in polymer chemistry; K.M.L. and W.L. contributed to the design of *in vivo* studies; N.J.G. and M.S.H. provided materials and technical expertise for the antigenicity studies; Y.Q., N.J.G., K.M.L., M.S.H., K.M. and A.C. analyzed and interpreted the results; Y.Q. and A.C. wrote the manuscript; and A.S., N.J.G., K.M.L., M.S.H., K.M. edited the manuscript. All authors discussed the results and commented on the manuscript.

Competing Financial Interests

A.C. and Y.Q. have a pending patent on the sortase-catalyzed C-terminal polymer conjugation technology (WO 2014194244 A1). M.S.H. is a co-inventor of Pegloticase (Krystexxa®) and receives royalties from sales of Pegloticase, along with his employer, Duke University.

Data Availability

The data that support the findings of this study are available in “figshare” with the identifier doi: 10.6084/m9.figshare.3976761 [54].

traditional PEGylated drugs, whose safety and efficacy are hindered by pre-existing anti-PEG antibodies in patients.

Introduction

With more than a hundred peptides and proteins approved by the FDA to treat various diseases and many more in clinical and pre-clinical development, therapeutic peptides and proteins are an important class of drugs today [1,2]. However, the clinical use of all peptides and most proteins (with the exception of antibodies, albumin [3] and transferrin [4]) is challenged by their short plasma half-life, necessitating frequent injections, which can cause an undesirable peak-to-valley fluctuation of the drug concentration *in vivo* as well as reduce patient compliance and increase treatment cost [5]. Other limitations of peptide and protein therapeutics may include poor stability, low solubility and immunogenicity [6]. To address these limitations, various delivery strategies have been developed for sustained delivery of peptide and protein therapeutics, ranging from particulate systems, depots, to chemical conjugation with long circulating polymers such as poly(ethylene glycol) (PEG), or recombinant fusions with long circulating proteins such as albumin or the Fc domain of antibodies [7,8].

PEGylation, or the covalent conjugation of therapeutic peptides and proteins, and more recently nucleotide-based drugs, with the “stealth” polymer PEG, is one of the most widely used approaches to increase the circulation half-life and stability and to reduce the immunogenicity of these therapeutic biomolecules, evident from the many PEGylated drugs approved by the FDA, and numerous others in development [6,9,10]. However, after close to four decades of research and over two decades of clinical use, the drawbacks of PEGylation have begun to emerge. Conventional methods for the synthesis of PEGylated conjugates have significant limitations: 1) conjugation involves the reaction between protein-repulsive PEG chains and biomacromolecules, so that even with a large excess of polymer, steric hindrance still results in a low yield of conjugate, typically in the 10–20% range [11]; 2) the presence of a large excess of unreacted polymer makes product purification non-trivial; and 3) conjugation typically involves reacting the chain-ends of the polymer with reactive side-groups on lysine and cysteine residues, which are often promiscuously distributed on the biomolecule, thus yielding chemically heterogeneous products that can significantly compromise the bioactivity of the drug and greatly complicate regulatory approval [12–15].

Furthermore, the immunogenicity of PEG has recently attracted much attention. Anti-PEG antibodies have been induced in patients treated with some PEGylated enzymes, and in clinical trials of PEG-uricase [16,17] and PEG-asparaginase [18], these anti-PEG antibodies have markedly accelerated blood clearance, abrogated clinical efficacy, and increased the risk and severity of infusion reactions. Circulating anti-PEG antibodies have also been found in individuals naïve to PEGylated materials, possibly induced by chronic exposure to free PEGs present in commonly used consumer products [19,20]. High levels of such pre-existing anti-PEG antibodies have recently been linked to serious first-exposure allergic reactions to a PEGylated RNA aptamer, which led to early termination of a clinical trial [21].

To address the synthetic limitations of previous PEG conjugation methodologies, we have previously developed a strategy named sortase-catalyzed polymer conjugation [22]. This strategy exploits the C-terminal native peptide ligation mechanism of the enzyme sortase A, derived from *Staphylococcus aureus*, to attach a polymerization initiator site-specifically and stoichiometrically (1:1) at the C-terminus of a peptide or protein, to enable grafting of the PEG-like brush polymer poly[oligo(ethylene glycol) methyl ether methacrylate] (POEGMA) from the peptide/protein macroinitiator by *in situ* Atom Transfer Radical Polymerization (ATRP) in aqueous buffer [23,24].

Although POEGMA has been grafted from various model proteins and peptides [22,25–29], very few studies to date have reported POEGMA conjugates of clinically relevant biologic therapeutics for systematic evaluation of the therapeutic potential of this class of conjugates, and conjugation was either carried out post-polymerization [30] or was non-specific [31]. Using our sortase-catalyzed polymer conjugation strategy, we grafted POEGMA site-specifically (C-terminal) and stoichiometrically (1:1) from exendin-4 (exendin), a peptide drug that is clinically used to treat type 2 diabetes [32]. We show that a single subcutaneous (s.c.) injection of exendin-C-POEGMA reduces blood glucose for 120 h in fed mice, which is 20 times longer than injection of the unmodified peptide. Most intriguingly, we show that breaking up and appending PEG as short oligomeric side-chains of optimized length on the conjugated POEGMA not only retains the long circulation of the POEGMA conjugates, but equally importantly eliminates their reactivity toward patient-derived PEG antibodies. These results demonstrate that the architecture of PEG appended to a biologic drug plays an important role in modulating its antigenicity. This finding is of particular clinical significance given the growing prevalence of pre-existing anti-PEG antibodies in the general population that is increasingly undermining the safety and efficacy of PEGylated therapeutics. Note in this article, the terms “antigenicity” and “immunogenicity” are not interchangeable. “Antigenicity” is defined herein as the reactivity of an antigen toward pre-existing antibodies in patients, whereas “immunogenicity” refers to the intrinsic ability of an antigen to generate antibodies in the body.

Results

Sortase-catalyzed C-terminal initiator attachment to exendin

We exploited the C-terminal native peptide ligation mechanism of sortase A to site-specifically attach the ATRP initiator N-(2-(2-(2-(2-aminoacetamido)acet-amido)acetamido) ethyl)-2-bromo-2-methylpropanamide (AEBMP) to the C-terminus of exendin (Fig. 1). A quaternary fusion protein, abbreviated as “exendin-srt-His_6-ELP”, was recombinantly expressed to serve as the sortase A substrate (Fig. 1a). As explained in an earlier study [22], “srt” stands for the native sortase A recognition sequence “LPETG” [33] and ELP refers to a stimulus-responsive elastin-like polypeptide that was incorporated to enable easy purification of the fusion protein by inverse transition cycling (ITC, Supplementary Fig. S1a), a nonchromatographic protein purification method that we previously developed [34]. The recognition sequence was deliberately located between the protein and the ELP, so that transpeptidation by sortase A not only attaches the initiator to exendin, but also conveniently liberates the purification tag. Sortase A with an N-terminal hexahistidine tag (His_6-tag) was

recombinantly expressed from a plasmid constructed in the earlier study [22] and was purified by immobilized metal affinity chromatography (IMAC, Supplementary Fig. S1b). The ATRP initiator AEBMP (Fig. 1) was chemically synthesized with an N-terminal $(Gly)_3$ motif serving as the nucleophile, as maximum reaction rates for sortase-catalyzed C-terminal ligation have been reported with two or more glycines [35].

Successful sortase-catalyzed initiator attachment (Fig. 1b) resulted in cleavage of exendin-LPETG-His_6-ELP into exendin-LPET and G-His_6-ELP, followed by attachment of AEBMP to exendin-LPET to generate the macroinitiator product (exendin-C-Br). Sodium dodecyl sulfate-polyacrylamide gel electrophoresis (SDS-PAGE) analysis of the reaction mixture (Fig. 2a) showed > 90% conversion to exendin-C-Br, as assessed by gel densitometry. Similar to the previous study [22], a His_6-tag was intentionally inserted between "srt" and ELP on the exendin-srt-His_6-ELP fusion, such that upon transpeptidation by His_6-sortase A, all the residual reactants, enzyme and side-products except the desired product —exendin-C-Br — carried a His_6-tag. Consequently, elution through an IMAC column yielded pure exendin-C-Br (Fig. 2a) in the eluent while leaving all other unwanted species bound to the resin.

Synthesis and characterization of exendin-C-POEGMA conjugates

Next, *in situ* Activator Regenerated by Electron Transfer (ARGET) ATRP [36] was carried out to graft POEGMA from exendin-C-Br (Fig. 1c). An OEGMA monomer with an average mass of ~500 Da or ~9 side-chain EG repeats (EG9) was used, as shown by liquid chromatography electrospray ionization mass spectrometry (LC/ESI-MS) analysis (Supplementary Fig. S2a). The reaction time was varied to produce EG9 exendin-C-POEGMA conjugates with a range of MWs. Size exclusion chromatography (SEC) analysis of exendin-C-Br before polymerization detected by UV-vis absorbance at 280 nm (Fig. 2b) showed a single peak eluting at 23.7 min. After polymerization, the intensity of the macroinitiator peak greatly diminished, and was accompanied by the appearance of peaks at 21.3, 19.5, 17.8, 16.5 and 15.0 min, corresponding to EG9 exendin-C-POEGMA conjugates with increasing MWs as the reaction time was increased. The results from UV-vis detection were in agreement with those from refractive index (RI) detection (Supplementary Fig. S3a). Integration of peak areas in the UV-vis chromatograms showed that the average conjugation yield was ~ 80%. As shown in Table 1, the synthesized conjugates had M_ns that ranged from 25.4 to 155.0 kDa and all conjugates had very narrow dispersities ($Đ \leq 1.15$). The conjugates could be easily and completely purified by a single round of preparative SEC (Supplementary Fig. S3b).

Exendin acts by binding and activating the G protein-coupled GLP-1 receptor (GLP-1R), which results in the release of cyclic adenosine monophosphate (cAMP) as a second messenger in a downstream signaling cascade, ultimately leading to secretion of insulin to regulate blood glucose [37]. The potency of native exendin and the EG9 exendin-C-POEGMA conjugates were next assessed by quantifying intracellular cAMP release as a result of GLP-1R activation in baby hamster kidney (BHK) cells that were stably transfected with rat GLP-1R. As shown in Fig. 2c and Table 1, grafting EG9 POEGMA from exendin increases the EC_{50} of the peptide in an overall MW-dependent manner, which indicates decreased

receptor binding with increasing polymer MW as a result of the steric hindrance imposed by the appended POEGMA chain.

In vivo therapeutic efficacy of EG9 exendin-C-POEGMA

The *in vivo* efficacy of EG9 exendin-C-POEGMA conjugates was assessed in male C57BL/6J mice that were maintained on a 60 kCal% fat diet, so as to develop a diabetic phenotype [38,39]. A dose-dependent study was first performed to determine an adequate dose. A 66.2 kDa EG9 exendin-C-POEGMA conjugate was administered into mice via a single s.c. injection at 25, 50 and 85 nmol/kg mouse body weight of the conjugate. Fed blood glucose levels measured at various time points post-injection revealed an overall slight increase in the duration of glucose reduction with increasing dose of the conjugate compared to phosphate buffered saline (PBS) control (Supplementary Figs. S4a and b, Table S1). A similar trend was observed in the mouse body weights, where the mice treated with the highest dose showed considerably more weight loss than the two lower doses (Supplementary Fig. S4c). While the weight-lowering benefit of exendin has been well established [40], overdosing can cause nausea, which can lead to acute weight loss in rodents [41]. The excessive weight loss seen in mice that received the highest dose suggests the possibility of nausea, and all subsequent studies were hence carried out with a dose of 25 nmol/kg.

To investigate the effect of MW on the glucose regulatory effect of EG9 exendin-C-POEGMA conjugates, native exendin and conjugates of four different MWs (M_n = 25.4, 54.6, 97.2 and 155.0 kDa) were tested at a single s.c. injection at 25 nmol/kg mouse body weight. While unmodified exendin was only able to lower blood glucose for 6 h relative to PBS control (Fig. 3a, full glucose profiles in Supplementary Fig. S5), modification with EG9 POEGMA significantly extended the glucose-lowering effect of exendin for up to 120 h, with a MW-dependence on the onset, magnitude and duration of the effect (Figs. 3b–e, Supplementary Table S2). As is evident from the overlaid glucose profiles in Supplementary Fig. S6a (overlaid un-normalized glucose profiles in Supplementary Fig. S6b), an increase in MW delays the onset but prolongs the duration of glucose reduction, and the two higher MW conjugates showed an overall smaller magnitude of glucose reduction. This trend is mirrored by the weight profiles of treated animals as well (Supplementary Fig. S6c). The two higher MW conjugates also showed much more flat and steady glucose profiles. The glucose profile of the 155.0 kDa conjugate in particular resembled that of a sustained release depot, with no peak-to-valley effect that can cause undesirable side effects.

The *in vitro* cAMP results and the *in vivo* MW-dependent fed glucose measurements collectively show that an increase in MW of the conjugated polymer decreases the potency but increases the circulation duration of the EG9 exendin-POEGMA conjugate. Therefore, we hypothesize that there exists an optimal MW of the conjugate that best balances these two opposing effects. The area under the curve (AUC) of the fed glucose profiles with respect to 0% baseline signifies total glucose exposure, which accounts for both the magnitude and duration of glucose reduction, and is therefore a manifestation of the combined effect of the two opposing factors. Plotting the AUC of fed glucose levels as a function of conjugate M_n indeed yielded a roughly inverted bell-shaped distribution with a

minimum at 54.6 kDa (Fig. 3f). This suggests that the 54.6 kDa conjugate is the optimal among the tested EG9 conjugates in terms of balancing receptor activation potency and sustained duration of action. We thus investigated the 54.6 kDa EG9 conjugate further in subsequent experiments.

To validate the results from the fed glucose measurements and to obtain further evidence of the efficacy of EG9 exendin-C-POEGMA conjugates, an intraperitoneal glucose tolerance test (IPGTT) was performed 24 h and 72 h after a single s.c. injection of the 54.6 kDa EG9 conjugate or unmodified exendin at 25 nmol/kg. IPGTT confirmed the prolonged presence of the conjugate in circulation and its significant effect on glycemic control: at 24 h post-injection, the AUC of blood glucose level over 2 h after glucose challenge is reduced by 68% ($P < 0.0001$, Fig. 4a), and at 72 h post-injection, the AUC is reduced by 48% for conjugate-treated mice compared with PBS controls ($P < 0.01$, Fig. 4b). This is in stark contrast to the unmodified exendin group, which was insignificant at both time points (Figs. 4c and d).

Antigenicity of EG9 exendin-C-POEGMA conjugates

We tested the reactivity of the 54.6 kDa EG9 exendin-C-POEGMA conjugate to anti-PEG antibodies in plasma samples of patients previously treated with PEGylated proteins using enzyme-linked immunosorbant assay (ELISA). In a direct ELISA, the 54.6 kDa EG9 exendin-C-POEGMA conjugate and various controls, including two FDA-approved drugs, Adagen® — a PEGylated adenosine deaminase for treating severe combined immunodeficiency disease (SCID) and Krystexxa® — a PEGylated uricase for treating chronic refractory gout, were directly coated on a plate and probed with diluent, an anti-PEG negative patient plasma sample or one of two anti-PEG positive patient plasma samples. As shown in Fig. 5a, while the EG9 exendin-C-POGEMA conjugate did show a small amount of binding to anti-PEG antibodies in the positive plasma samples, the extent of binding is significantly less than those of the two PEGylated positive controls. This result was confirmed by a competitive ELISA, where Krystexxa® was coated on wells, and different amounts of 54.6 kDa EG9 exendin-C-POEGMA and controls were added in solution to compete for binding to anti-PEG antibodies in an anti-PEG positive plasma sample. As can be seen in Fig. 5b, at all tested competing antigen amounts, 54.6 kDa EG9 exendin-C-POEGMA showed significantly reduced antibody binding compared to the positive control, Adagen®.

Exendin-C-POEGMA with shorter side-chain length

These results led us to hypothesize that the reduced PEG antigenicity of the EG9 exendin-C-POEGMA conjugate is due to both the branched architecture and the short side-chain length of the conjugated POEGMA. As a minimum length of PEG is presumably needed for antibody recognition and binding [42], we hypothesized that optimizing the side-chain OEG length may further reduce or possibly eliminate the antigenicity of POEGMA conjugates to anti-PEG antibodies. To test this hypothesis, we next synthesized exendin-C-POEGMA conjugates using OEGMA monomer with precisely 3 EG side-chain repeats as seen by LC/ESI-MS (Supplementary Fig. S2b), as evidence in the literature suggests that the antigenic determinant of PEG may be ~6–7 EG repeats [42]. Three different EG3 exendin-C-POEGMA

conjugates with M_ns of 26.3, 55.6, and 71.6 kDa (Table 1) were synthesized. Assessment of conjugate potency by intracellular cAMP ELISA (Supplementary Fig. S7) showed that similar to the EG9 conjugates, conjugation of EG3 POEGMA to the C-terminus of exendin caused an increase in the EC_{50} (Table 1), indicating a decrease in the receptor activation of the conjugates, though with a less pronounced MW-dependence.

Antigenicity and efficacy of EG3 exendin-C-POEGMA conjugates

We next tested the reactivity of a 55.6 kDa EG3 exendin-C-POEGMA conjugate to anti-PEG antibodies in patient plasma samples. The 54.6 kDa EG9 conjugate was included as a control to confirm the repeatability of the assays. Remarkably, both direct and competitive anti-PEG ELISAs (Figs. 5c and d) showed that reducing the side-chain length of the conjugated POEGMA down to 3 EG repeats completely eliminated the reactivity of the conjugate toward anti-PEG antibodies present in the patient plasma samples.

As the OEG side-chains on POEGMA are largely responsible for the “stealth” behavior of the polymer and its conjugates, alteration on the side-chain length can thus have an impact on the *in vivo* behavior of POEGMA conjugates. Therefore, we next investigated the *in vivo* efficacy of EG3 exendin-C-POEGMA. The 55.6 kDa and 71.6 kDa EG3 exendin-C-POEGMA conjugates were administered into fed mice via a single s.c. injection at 25 nmol/kg mouse body weight. As can be seen from the post-injection glucose profiles in Figs. 6a and b (unnormalized glucose profiles and weight profiles in Supplementary Fig. S8), both conjugates significantly reduced mouse blood glucose for up to 96 h compared to PBS control. The EG3 conjugates appear to have slightly lower magnitudes of glucose reduction and more flat glucose profiles compared to their EG9 counterparts.

Pharmacokinetics of exendin-C-POEGMA conjugates

To further confirm the prolonged circulation of exendin-C-POEGMA conjugates and to seek some answers to the difference between the glucose profiles of EG9 and EG3 conjugates, a pharmacokinetics study was performed with fluorescently labeled exendin, the 54.6 kDa EG9, 55.6 kDa EG3 and 71.6 kDa EG3 conjugates. Two MWs of the EG3 conjugate were tested, as the EG3 and EG9 conjugates have different R_hs at the same MW. The MWs were chosen such that the 54.6 kDa EG9 conjugate (R_h = 5.4±0.6 nm) has similar MW as the 55.6kDa EG3 conjugate and similar R_h as the 71.6 kDa EG3 conjugate (R_h = 5.6±0.5 nm). The plasma concentration-time courses (Figs. 6c and d) were analyzed using a non-compartmental fit characterizing the absorption and elimination phases of the pharmacokinetic profiles, to approximate the parameters shown in Table 2.

After s.c. injection, unmodified exendin had a very short residence time in circulation, with a rapid absorption phase ($t_{1/2a}$ = 0.7±0.1 h) and a short terminal elimination phase ($t_{1/2el}$ = 1.7±0.2 h). In contrast, the exendin-C-POEGMA conjugates tested increased the absorption time by ~ 9 to 13-fold, with the two EG3 conjugates taking longer than the EG9 conjugate to absorb into circulation. Similarly, the 54.6 kDa EG9 conjugate prolonged the elimination phase of exendin by ~ 25-fold, while the two EG3 conjugates afforded a bigger increase of ~36-fold. These differences in the pharmacokinetics resulted in ~ 20-fold increase in AUC for the conjugates compared to unmodified exendin, indicating that conjugation of

POEGMA to the C-terminus of exendin significantly enhanced the cumulative exposure of the peptide in circulation. While the C_{max} of the two EG3 conjugates were considerably lower than that of the EG9 conjugate, consistent with the lower magnitude of glucose reduction seen for the EG3 conjugates in the fed blood glucose studies (Figs. 6a and b), the AUC of the three tested conjugates were comparable given the longer absorption and elimination half-lives of the EG3 conjugates.

Discussion

Using our previously developed sortase-catalyzed polymer conjugation strategy [22], we synthesized site-specific (C-terminal) and stoichiometric (1:1) exendin-C-POEGMA conjugates with an average overall yield of up to > 70%, which compares favorably to the 10–20 % overall yield often seen in conventional PEGylation processes [11]. The small fraction of unreacted exendin-C-Br in the *in situ* ATRP reactions is likely due to hydrolysis or disproportionation at the C-terminus of the macroinitiator, which are common side-reactions of ATRP in aqueous conditions that lead to loss of the Br functionality and thus inactivation of the macroinitiator [43]. Additionally, as a controlled radical polymerization technique, ATRP enabled synthesis of conjugates with a wide and tunable range of MWs and very narrow MW distributions. Together, our synthesis approach gives rise to polymer conjugates of therapeutic biomolecules that are far more homogeneous than PEGylated drugs currently in clinical use. This full control over site and stoichiometry of conjugation, and high degree of MW tunability and low dispersity are highly desirable features for polymer conjugates of therapeutic biomolecules, as they translate to a more predictable therapeutic performance.

EG9 exendin-C-POEGMA conjugates lowered blood glucose levels in fed mice for up to 20 times longer than unmodified exendin injected at the same dose. This prolonged duration of therapeutic effect significantly reduces the required administration frequency, a benefit critical to a disease whose treatment outcomes rely heavily on patient compliance. The fed blood glucose study of the EG9 conjugates showed that an increase in MW was correlated with a slower onset of glucose reduction and the two higher MW conjugates showed an overall smaller magnitude of glucose reduction. These are speculated to be due in part to the reduced receptor binding activity and also perhaps a retarded diffusion from the subcutaneous space into systemic circulation affected by an increase in conjugate size.

The trends observed in fed blood glucose levels are also evident in mouse body weight profiles. A drop in body weight at the beginning of the study is expected for all mice including the PBS control group, as the mice are subjected to stress factors including injection and repetitive tail vein glucose measurements. This stress-induced response is also evident in the sharp spike in their glucose levels at the initial time points. The PBS group in the fed blood glucose measurement study of the 71.6 kDa EG3 exendin-C-POEGMA conjugate had a more pronounced weight drop than in the other fed glucose studies. This is likely due to the fact that mice in these studies were fed a 60 kcal% fat diet, which makes them metabolically less stable and weight variations are thus more common. The slightly bigger weight loss of the PBS group in this particular experiment is consistent with a more

sustained initial increase in blood glucose, suggesting that this batch of mice reacted more strongly to the procedural stress.

Two critical —and opposing— features of protein-polymer conjugates that are clearly illustrated by this study are the inverse relationship between conjugate MW and potency versus circulation duration. Up to a threshold, the MW of the conjugate is expected to be directly proportional to the circulation duration but inversely proportional to the receptor-binding activity of the biomolecule of interest. Indeed plotting the AUC of blood glucose profiles of the tested EG9 exendin-C-POEGMA conjugates as a function of conjugate M_n, which accounts for both the magnitude and duration of glucose reduction, gives an inverted bell-shaped distribution with a minimum at 54.6 kDa, suggesting that the 54.6 kDa conjugate is the optimal among the tested conjugates in terms of balancing receptor activation potency and sustained duration of action. The result also suggests that the renal clearance threshold for these EG9 conjugates is between 25.4 and 54.6 kDa, as although the 25.4 kDa conjugate is more potent than the 54.6 kDa conjugate *in vitro*, its overall glucose lowering effect is smaller than that of the 54.6 kDa conjugate and its effect also diminished more quickly, which points to a much faster renal clearance.

The antigenicity of EG9 exendin-C-POEGMA conjugates, or their reactivity toward pre-existing anti-PEG antibodies in patients, was of particular interest because the serious consequences of PEG immunogenicity have become increasingly apparent. Anti-PEG antibodies have been induced in patients treated with PEGylated drugs and have been shown to correlate with rapid clearance of these drugs [16–18]. High levels of pre-existing anti-PEG antibodies have also been found in individuals naïve to PEGylated agents, which are associated with serious and sometimes life-threatening first-exposure allergic reactions [21]. Therefore, it is of high clinical relevance to prescreen polymer conjugates of therapeutic peptides and proteins for antigenicity toward anti-PEG antibodies.

We found that the 54.6 kDa EG9 exendin-C-POEGMA conjugate showed significantly less reactivity toward anti-PEG antibodies in patient plasmas compared to two FDA-approved drugs, Adagen® and Krystexxa®. More intriguingly, reducing the side-chain length of the conjugated POEGMA to 3 EG repeats completely eliminated antibody binding. We speculate that the complete elimination of anti-PEG antigenicity of EG3 POEGMA has two potential molecular explanations. First, three ethylene glycol repeats may be shorter than the epitope recognized by anti-PEG antibodies, which is consistent with a pervious report that the antigenic determinant of PEG may be 6–7 repeat units [42]. Second, distributing PEG as oligomeric side-chains may create a “stacking effect” that hinders antibody access. Given that POEGMA is not currently present in any pharmaceutical or consumer product, it is reasonable to speculate that humans would not have any pre-existing antibodies to the polymer. Thus clinically, the lack of anti-PEG antigenicity of POEGMA conjugates is expected to translate to complete elimination of serious and sometimes life-threatening first-exposure allergic reactions in patients toward POEGMA conjugates of therapeutics, and should eliminate the accelerated blood clearance of POEGMA-drug conjugates due to pre-existing anti-PEG antibodies in patients. We believe this is a particularly timely and useful finding that will address the pressing problem of increasing level of pre-existing anti-PEG antibodies in the general population that is compromising the safety and efficacy of FDA-

approved PEGylated drugs and hindering the progress of other PEG conjugates in clinical and pre-clinical development. Given that PEGylation remains the most widely used technology clinically to extend the half-life and improve the bioavailability of biologic drugs, a method to tackle the emerging problem of antigenicity of PEG by modulation of its architecture —from linear to branched—provides a new approach to solve this problem. We note that this study addresses the anti-PEG antigenicity of POEGMA conjugates of biologic drugs, but does not make any claims about their intrinsic immunogenicity. While immunogenicity is also a crucial aspect regarding the safety of this class of conjugates, a thorough investigation will involve extensive *in vivo* studies performed in multiple species that is beyond the scope of this study.

Fed glucose measurement study confirmed that elimination of antigenicity did not occur at the cost of *in vivo* efficacy. While the magnitude of glucose reduction of the EG3 conjugates is slightly lower than that of the EG9 conjugates, the glucose profiles resemble that of a sustained release depot, with no peak-to-valley effect often associated with parenteral drug administration that can cause unwanted side effects. Pharmacokinetic comparison of the 55.6 kDa and 71.6 kDa EG3 conjugates with the 54.6 kDa EG9 conjugate showed that while the C_{max} values of the EG3 conjugates were smaller than that of the EG9 conjugate, their longer absorption and elimination half-lives gave rise to comparable AUCs as that of the EG9 conjugate. This finding is consistent with the more flat and steady glucose profiles of the EG3 conjugates. We speculate that the relatively higher hydrophobicity of EG3 POEGMA may cause its conjugates to remain in the s.c. space or lodge in other tissues during their course in circulation for more extended periods of time, thus creating a depot-like effect.

POEGMA was polymerized from the C-terminus of exendin in this study because the N-terminus of the peptide is important for GLP-1R binding and activation [37]. We note that while we have demonstrated utility of the sortase-catalyzed C-terminal polymer conjugation strategy with exendin in this study, it is a generally applicable platform for improving the pharmacological performance of therapeutic proteins and peptides where the C-terminus is not essential for the activity of the biomolecule. For other biologics where the C-terminal end may be critical to its activity, we have developed a complementary N-terminal approach [26]. In the event that both N- and C-termini of the peptide/protein are critical to its activity, methods developed by us and other investigators can be used for site-specific incorporation of an ATRP initiator at solvent-accessible sites within the primary amino acid sequence of the peptide or protein drug [44,45]. These methods collectively offer a general toolbox that should enable site-specific POEGMA conjugation at any desired solvent-accessible site on a peptide or protein.

Collectively, our results establish site-specific POEGMA conjugation as a next-generation PEGylation technology that is highly useful for improving the pharmacological performance of therapeutic biomolecules while providing a solution to the increasing levels of pre-existing anti-PEG antibodies in patients that limit the safety and efficacy of traditional PEGylated drugs. While these results are promising, we believe that a deeper understanding of the mechanism of action, efficacy and safety of exendin-C-POEGMA conjugates, particularly the EG3 variants, is necessary for clinical translation. Future plans include

optimizing the MW of EG3 exendin-C-POEGMA conjugates to maximize efficacy, measuring insulin release, investigating the *in vivo* biodistribution of the conjugates, and studying long-term parameters of therapeutic efficacy such as hemoglobin A1c (HbA1c), glycated albumin and pancreatic β-cell proliferation to understand the long-term therapeutic potential of exendin-C-POEGMA conjugates. Furthermore, assessment of the intrinsic immunogenicity of exendin-C-POEGMA conjugates is essential to ensure their long-term safety and efficacy for clinical translation.

Methods

Experimental Design

All *in vitro* and *in vivo* experiments include suitable controls; where applicable, PBS served as a negative control and unmodified exendin served as a positive control. The sample sizes for *in vivo* studies were chosen based on similar studies conducted previously [46,47]. See *Animal studies* section below for details on the animal model used. Mice were randomly grouped before initiation of each experiment. The investigator was not blinded to group allocation. For the *in vivo* fed glucose measurement studies, mouse blood glucose levels were measured until all experimental groups no longer showed statistical significance in glucose reduction compared to the PBS control group. All collected data points were included in data analysis.

Cloning, expression and purification

All molecular biology reagents were purchased from New England Biolabs unless otherwise specified. The gene encoding exendin in a pMA-T vector was codon optimized and synthesized by Life Technologies. The first methionine residue encoding the translational start codon in proteins recombinantly expressed in *E. coli* needs to be cleaved post-translationally for proper function and stability of the protein [48]. However, the first amino acid of exendin is a histidine, and our past experience and reports in the literature [48] both suggest that having histidine as the residue immediately following methionine prevents proper methionine cleavage. Thus, a di-alanine leader was incorporated at the N-terminus of the peptide to facilitate methionine cleavage. Once *in vivo*, the di-alanine leader can be cleaved by dipeptidyl peptidase 4 (DPP4), an exopeptidase that cleaves N-terminal dipeptides containing proline or alanine as the second residue, to reveal the N-terminus of exendin for GLP-1R binding. The exendin gene was amplified by polymerase chain reaction (PCR), using forward and reverse primers containing NdeI overhangs and with the sequence for the sortase A recognition motif “LPETG” (named “srt” for brevity) followed by a His_6-tag incorporated in the reverse primer. The amplified “exendin-srt-His_6” fragment was inserted into a modified pET-24a+ vector [49] at an NdeI restriction site immediately upstream of an ELP with the sequence $(VPGVG)_{60}$, to yield “exendin-srt-His_6-ELP”.

Expression and purification of the quaternary fusion protein followed previously described procedures with minor changes [22]. Briefly, cells were cultured in Terrific Broth (TB, Mo Bio Laboratories, Inc.) supplemented with 45 μg/ml of kanamycin at 25 °C. Once the optical density at 600 nm (OD_{600}) of the culture reached 0.6, temperature was lowered to 16 °C and isopropyl β-D-1-thiogalactopyranoside (IPTG, AMRESCO) was added to a final

concentration of 0.1 mM to induce protein expression. Cells were harvested 15 h post induction by centrifugation at 700×g for 10 min and were lysed by sonication on a Misonex Ultrasonic Liquid Processer (Qsonica, LLC.) at amplitude 85 for 3 min with 10 sec on and 40 sec off cycles. Nucleic acids were removed from the crude extract by addition of 1 vol % polyethyleneimine (PEI, Acros) followed by centrifugation at 4 °C and 21,000×g for 10 min. The ELP tag enables purification of the fusion protein by ITC, a nonchromatographic method that we have previously developed for the purification of ELP fusion proteins that takes advantage of the inverse phase transition behavior imparted by the ELP [34]. After triggering the inverse phase transition of the fusion by addition of 0.1 M ammonium sulfate, the aggregated proteins were collected by centrifugation at ~30 °C and 21,000×g for 10 min. The pellet was then resolubilized in cold PBS and the resulting solution was centrifuged at 4 °C and 21,000×g for 10 min to remove any remaining insoluble material. The last two steps were typically repeated one more time to obtain homogeneous protein, as verified by SDS-PAGE. In the final step, the protein was resolubilized in sortase buffer (50 mM Tris, 150 mM NaCl, 10 mM $CaCl_2$, pH adjusted to 7.5) in preparation for sortase-catalyzed initiator attachment.

The gene for sortase A with a 59 N-terminal amino acid truncation (previously shown to not affect its transpeptidase activity [50]) and an N-terminal His6-tag in a pET15b vector was available from a previous study. Expression and purification of His_6-sortase A were carried out as previously described [22].

Sortase-catalyzed initiator attachment and macroinitiator purification

The exendin-C-Br macroinitiator was synthesized and purified following procedures described previously with minor changes [22]. Briefly, a reaction mixture consisting of exendin-srt-His_6-ELP, His_6-sortase A, and AEBMP at a 2:1:60 ratio in sortase buffer was incubated at 20 °C for 18 h. After reaction, a reverse His-tag purification was used to isolate the exendin-C-Br macroinitiator, by exploiting the fact that it is the only species in the mixture without a His_6-tag. Purification was performed on an AKTA Purifier (GE Healthcare) equipped with a photodiode detector set at 280 nm and a HisTrap HP column. Elution through the column with PBS yielded pure exendin-C-Br in the eluent while leaving all other unwanted species bound to the resin. The collected exendin-C-Br was dialyzed overnight in PBS (pH 7.4) to remove residual free initiator.

Macroinitiator characterization

MALDI-MS was performed on a Voyager-DE Pro mass spectrometer (Life Technologies). Samples at ~25 μM in PBS were diluted 1:10 with 10 mg/mL sinapinic acid in 90:10 water/acetonitrile with 0.1 vol % trifluoroacetic acid (TFA) as the ionization matrix. The instrument was operated in linear mode with positive ions generated using a N_2 laser. Ubiquitin was used as a molecular weight standard to calibrate the instrument.

For LC/MS-MS analysis to confirm site-specificity of initiator attachment, 100 μL of ~8 uM exendin-C-Br in PBS was solvent exchanged into 50 mM ammonium bicarbonate (pH 8.0) on a ZebaSpin desalting column (Thermo Fisher Scientific) followed by trypsin (sequencing grade, Promega) digestion at 37°C for 18 h directly in the column. The digestion mixture

was collected by centrifugation, dried by vacuum centrifugation and was then resuspended in 20 μL 2% acetonitrile and 0.1% formic acid in water. 1 μL of the sample was separated on a NanoAquity ultra performance liquid chromatography (UPLC, Waters) system equipped with a BEH130 C18 reversed phase column (Waters) using a mobile phase consisting of (A) 0.1% formic acid in water and (B) 0.1% formic acid in acetonitrile. A linear gradient of 5% B to 40% B was performed over 60 min at 400 nL/min and the separated peptides were ionized by electrospray ionization (ESI) followed by MS analysis on a Synapt G2 HDMS QToF mass spectrometer (Waters). The top four most abundant ions were selected for MS/MS. Mass spectra were processed with Mascot Distiller (Matrix Science) and were then submitted to Mascot searches (Matrix Science) against a SwissProt_Ecoli database appended with the custom exendin-C-Br sequence. Search results were imported into Scaffold (v4.0, Proteome Software) and scoring thresholds were set to yield a minimum of 99% protein confidence for protein identification. Extracted ion chromatograms were performed in MassLynx (v4.1). Experimental isotope distributions of the brominated C-terminal tryptic peptide was compared to a theoretical isotope distribution modeled in Molecular Weight Calculator (v. 6.49, Pacific Northwest National Laboratory, ncrr.pnl.gov/software).

In situ ARGET-ATRP

All chemical reagents were purchased from Sigma Aldrich and used as received, unless otherwise specified. EG9 OEGMA monomer (M_n ~500 Da or ~9 side-chain EG repeats on average, Sigma Aldrich, #447943) and EG3 OEGMA monomer (triethylene glycol methyl ether methacrylate, 232 Da, Sigma Aldrich, #729841) were passed through a column of basic alumina to remove the inhibitors.

In a typical reaction, 216 μmol of OEGMA and 21.6 μL of a stock solution of 200 mM $CuBr_2$ and 1.6 M tris(2-pyridylmethyl)amine (TPMA) pre-complexed in MilliQ water with 5% dimethylformamide (DMF) were mixed with 1 mL of 500 μM exendin-C-Br in PBS in a Schlenk flask. A 3.2 mM solution of ascorbic acid in MilliQ water was prepared in a separate flask. The two solutions were degassed by bubbling with argon for 30 min, after which Activator-Regenerated Electron Transfer (ARGET) ATRP was initiated and maintained by continuously injecting the ascorbic acid solution into the reaction medium using a syringe pump at a rate of 1.6 nmol/min. Polymerization was allowed to proceed for a specified time at 20 °C under argon and was quenched by bubbling with air. Reactions of the EG3 OEGMA were done with 443 μmol of the monomer in 20 v/v% methanol in PBS while all other conditions remained the same. At the end of the reaction, the reaction mixture was dialyzed against PBS overnight to remove residual small molecule reagents in preparation for downstream characterization and purification.

Characterization of OEGMA monomers

Monomers diluted 1:20,000 in methanol were separated on an Agilent 1100 LC system equipped with a Zorbax Eclipse Plus C18 column (Agilent) using a mobile phase consisting of (A) 0.3% formic acid in water and (B) 0.3% formic acid in acetonitrile. A linear gradient of 50% B to 95% B was performed over 10 min at 50 °C. Separated samples were ionized by ESI followed by MS analysis on an Agilent MSD ion trap mass spectrometer.

Physical characterization of exendin-C-POEGMA conjugates

Analytical SEC was performed on a Shimadzu high performance liquid chromatography (HPLC) system equipped with a UV-vis detector (SPD-10A VP) operating at 280 nm. 50 μL of samples at ~2 mg/mL were separated on a Protein KW-803 column (Shodex) using 0.1M Tris-HCl (pH 7.4) as mobile phase at 25 °C with a flow rate of 0.5 mL/min. Conjugation efficiency of *in situ* ATRP from exendin was calculated by quantifying AUC of peaks detected at 280 nm. Sum of the AUC's of the two peaks corresponding to the unreacted macroinitiator and the conjugate in each chromatogram was regarded as 100% and % fraction of the conjugate peak was calculated as the conjugation efficiency of that particular polymerization reaction.

The fluid line of the analytical HPLC system was connected downstream in series to a DAWN HELEOS II MALS detector followed by an Optilab T-rEX refractometer (both from Wyatt Technology) for conducting SEC-MALS analysis. The system was calibrated with toluene and normalized with 2.0 mg/mL bovine serum albumin (BSA, Pierce). Samples were passed through 0.1 μm filters before injection. dn/dc values of the conjugates were determined on an Anton Paar Abbemat 500 refractometer (Anton Paar). Data were analyzed in ASTRA (v. 6.0, Wyatt Technology) to compute M_w, M_n and $Đ$ of the conjugates.

Conjugates were purified by a single round of preparative SEC on an AKTA Purifier equipped with a photodiode detector set at 280 nm and a HiLoad 26/600 Superdex 200 PG column using PBS as mobile phase at 4 °C and a flow rate of 2.0 mL/min.

DLS was performed on a DynaPro Plate Reader (Wyatt Technology). Samples were prepared at 25 μM and filtered with 0.1 μm filters before analysis. The instrument was operating at a laser wavelength of 831.95 nm, a scattering angle of 90° and at 25 °C. Data were analyzed in Dynals mode using Dynamics 6.12.0.3.

General biochemical analysis

Concentrations of fusion proteins were measured on a ND-1000 Nanodrop spectrophotometer (Thermo Scientific) by UV-vis absorption spectroscopy. Concentration of exendin and conjugates for *in vitro* assays and *in vivo* studies was assessed using a Bicinchoninic Acid (BCA, Pierce) assay following manufacturer's instructions. SDS-PAGE analysis of sortase A was performed using precast 4–20% Tris-HCl gels (Bio-Rad). SDS-PAGE analyses of all exendin derivatives were performed using precast Tris/Tricine gels (Bio-Rad). Quantification of sortase reaction conversion was done by gel densitometry analysis using a built-in function in Image Lab (v. 4.0.1, Bio-Rad).

In vitro cAMP ELISA

Activity of native exendin and conjugates was assessed *in vitro* by quantifying intracellular cAMP release as a result of GLP-1R activation in BHK cells stably transfected with rat GLP-1R (a generous gift of Drucker group, University of Toronto, Toronto, Canada) [51]. Cells were allowed to reach 70–80% confluence in 24-well plates. Prior to the assay, ~20 μg of peptide or equivalent of conjugates were treated with 0.5 μg DPP4 (ProSpect) overnight to remove the di-alanine leader. On the day of the assay, cells were incubated with 3-

isobutyl-1-methylxanthineto (IBMX, EMD Millipore) for 1 h to prevent cAMP degradation [52], followed by incubation with varying concentrations (0.001–1000 nM in log-scale increments) of exendin (Genscript) or conjugates for 10 min to trigger GLP-1R activation. 0.1M HCl was then added to disrupt the cells and release intracellular cAMP. cAMP concentration was measured by a competitive cAMP ELISA according to the manufacturer's protocol (Enzo Life Sciences). Each sample was assayed in triplicate and data were analyzed in Igor Pro (v. 6.2, Wavemetrics) using a Hill equation fit to determine the EC50 of each construct [53].

Animal studies

In vivo experiments were performed with 6-week-old male C57BL/6J mice (stock no. 000664) purchased from Jackson Laboratories. Upon arrival, mice were initiated on a 60 kCal% fat diet (#D12492, Research Diets Inc.) to induce a diabetic phenotype. Previous studies have established high fat-fed C57BL/6J mice as an adequate model for type 2 diabetes, as after one week on a high-fat diet, mice exhibit elevated blood glucose, progressively increasing insulin level, and severely compromised insulin response and glucose tolerance [38,39]. Mice were housed under controlled light on a 12 h light/12 h dark cycle with free access to food and water. All mice were allowed to acclimate to the high-fat diet and the facility for 10 d before initiation of experiments. Mice used for fed glucose measurement study of EG3 conjugates were maintained on the high-fat diet for 3 weeks and used at the age of 8 weeks. All animal care and experimental procedures were approved by the Duke Institutional Animal Care and Use Committee.

In vivo fed glucose measurements

The effect of native exendin and the conjugates on fed blood glucose levels was measured following a single s.c. injection of each sample. Before blood glucose measurement, the tail was wiped with a sterilizing alcohol solution and wiped dry. A tiny incision was made on the mouse tail vein using a disposable lancet, and the first 1 μL drop of blood was wiped off. The second 1–2 μL blood drop was used for glucose measurement using a hand-held glucometer (AlphaTrack, Abbott). Blood glucose levels were measured 1 d before the experiment. On the day of injection, weights and blood glucose were measured, and a sample solution or PBS control of equivalent volume was injected s.c. Immediately following injection, mice were placed back in the cage with free access to food and water, and blood glucose was measured at 1, 4, 6 (exendin only), 8, 24, 48, 72, 96, 120 and 144 h post-injection. Weights were monitored daily. In the EG9 dose-dependent study, a 66.2 kDa EG9 exendin-C-POEGMA conjugate was injected into mice (n=3) at 25, 50, and 85 nmol/kg mouse body weight. In the EG9 MW-dependent study, EG9 conjugates of 25.4, 54.6, 97.2 and 155.0 kDa M_ns were injected into mice (n=6) at 25 nmol/kg. In the EG3 fed glucose study, 55.6kDa and 71.6 kDa EG3 exendin-C-POEGMA conjugates were injected into mice (n=5) at 25 nmol/kg. Blood glucose levels were normalized by the average glucose levels measured 24 h and immediately before injection to reflect the percent change in blood glucose and to correct for transient variations in glucose.

In vivo IPGTT

Mice were randomly divided into groups (n=5 in Figs. 4a and b, n=3 in Figs. 4c and d). On day one, every two groups of mice received a s.c. injection of either 54.6 kDa EG9 exendin-C-POEGMA conjugate, exendin as positive control, or PBS at equivalent volume as negative control. Exendin and the conjugate were injected at 25 nmol/kg. 18 h after injection, one group of mice in each category were fasted by removal of food for 6 h. At the end of the fast period (24 h following injection), mice were given 1.5 g/kg glucose (10 w/v % sterile glucose solution, Sigma) via i.p. injection. Blood glucose levels were monitored by nicking the tail vein and measuring the glucose level in the blood using a glucometer at 0, 20, 40, 60, 90, and 120 min after glucose administration. 66 h after injection, the remaining groups of mice were subjected to the same protocol and an IPGTT was similarly performed 72 h following injection.

In vivo pharmacokinetics

Exendin, 54.6 kDa EG9, 55.6 kDa EG3 and 71.6 kDa EG3 exendin-C-POEGMA conjugates were fluorescently labeled with Alexa Fluor® 488 NHS ester (Thermo Fisher Scientific) via their solvent accessible primary amines on lysine residues and the N-terminus, according to manufacturer's protocol. Unreacted free fluorophore was removed using a ZebaSpin desalting column (Thermo Fisher Scientific). Mice were randomly divided into four groups (n=3). Animals were weighed before injection. Each group of mice received a single s.c. injection of one of the labeled samples at 75 nmol/kg (45 nmol/kg fluorophore). 10 μL of blood samples were collected from the tail vein into 100 μL of a heparin solution (1kU/ml in PBS, Sigma Aldrich) at 40 s, 40 min, 2.5 h, 4.5 h, 8 h, 24 h, 48 h, 72 h, 96 h and 120 h after injection. Blood samples were centrifuged at 4 °C and 20,000 ×g for 10 min to extract the plasma for fluorescence reading at excitation 485 nm and emission 535 nm on a Victor multilabel plate reader (Perkin Elmer). Plasma concentrations of constructs as a function of time were fitted using a non-compartmental analysis (PK Solutions 2.0, Summit Research Services) that characterizes the absorption and elimination phases of the profiles to derive the pharmacokinetic parameters.

In vitro anti-PEG ELISA

In the direct ELISA, columns of a 96-well microtiter plate (CoStar) were coated with Krystexxa® (Crealta Pharmaceuticals), ADA (Sigma-Tau Pharmaceuticals), Adagen® (Sigma-Tau Pharmaceuticals), exendin (Genscript), a 54.6 kDa EG9 exendin-C-POEGMA conjugate, a 55.6 kDa EG3 exendin-C-POEGMA conjugate or BSA (Sigma Aldrich). The antigen solutions for plate coating were prepared in PBS to yield ~2 μg of unmodified peptide/protein or ~5 μg of PEG/OEG in the case of polymer-modified antigens per well upon adding 50 μL to each well. The PEG/OEG contents of the polymer-modified antigens were calculated as follows: Krystexxa® consists of the tetrameric uricase enzyme (125 kDa total) with 10–11 lysine side-chain amino groups on each of its four subunits reacted with 10 kDa PEG *p*-nitrophenyl carbonate ester [9], giving a PEG content of ~76%. Adagen® consists of ADA (40.8 kDa) with 11–17 of its side-chain amino groups on solvent-accessible lysines functionalized with 5 kDa monomethoxy succinyl PEG according to the manufacturer's specifications (Sigma-Tau Pharmaceuticals). For our calculation, we assumed 14 PEG

chains per Adagen® conjugate on average, giving ~60% PEG content. In the case of the exendin-C-POEGMA conjugates, subtracting the poly(methyl methacrylate) backbone (~17% for EG9 POEGMA and ~37% for EG3 POEGMA) gives an OEG content of ~75% for the 54.6 kDa EG9 conjugate and ~58% for the 55.6 kDa EG3 conjugate. After overnight incubation of the coated plate at 4 °C, it was washed with PBS and all wells were blocked with 1% BSA in PBS. One patient plasma sample previously tested negative for PEG antibody and two that were tested positive were diluted 1:400 v/v in 1% BSA in PBS. The two positive patient plasma samples were from two different individuals that developed anti-PEG antibodies during a Phase II clinical trial of Krystexxa®. Following another round of PBS washing, 100 μL of each diluted plasma sample and 1% BSA in PBS were added to replicate wells of each antigen. The plate was then incubated at room temperature for 2 h. Wells were again washed with PBS and 100 μL of alkaline phosphatase-conjugated goat anti-human IgG (Sigma) diluted 1:5250 with 1% BSA in PBS was added to each well. After 1 h incubation at room temperature, wells were washed with PBS followed by Tris-buffered saline. Bound alkaline phosphatase was detected by incubating with p-nitrophenyl phosphate (Sigma) in accordance with the directions of the supplier. The phosphatase reaction was stopped by adding 50 μL/well of 10% NaOH, and the absorbance at 405 nm was measured on a plate reader (Tecan Infinite M200 Pro, Tecan Austria).

In the competitive ELISA, a microtiter plate was coated with 50 μL of 100 μg/mL Krystexxa® per well by overnight incubation at 4 °C. Various amounts of ADA, Adagen®, exendin, a 54.6 kDa EG9 exendin-C-POEGMA conjugate, and a 55.6 kDa EG3 exendin-C-POEGMA conjugate were diluted with PBS to yield 0, 0.5, 2, 5, 10 and 20 μg of competing antigen per well upon adding 50 μL to each well. Dilutions of Adagen® and the exendin-C-POEGMA conjugates were prepared such that at each competing antigen concentration, similar PEG/OEG contents were compared as shown in Table S3. The diluted competing antigens were mixed with equal volume of a patient plasma sample that tested positive for PEG antibody (diluted 1:200 v/v in 1% BSA in PBS) and incubated at 4 °C overnight. The following morning, after washing with PBS, all wells were blocked with 1% BSA in PBS. Wells were washed with PBS after blocking, and 100 μL of each concentration of the competing antigen-plasma mixtures was added in replicate wells. After incubation at room temperature for 2 h, alkaline phosphatase-conjugated IgG was added for colorimetric readout at 405 nm as described above.

Assays in Figs. 5a and 5b were performed with n=3, while those in Figs. 5c and 5d were performed with n=5.

Statistical analysis

Data are presented as means ± standard errors (SEs). Blood glucose levels in fed glucose measurement studies (n=6) were normalized by the average glucose levels measured 24 h and immediately before injection. Treatment effects on fed glucose levels were analyzed using repeated measures two-way ANOVA, followed by *post hoc* Dunnett's multiple comparison test to evaluate individual differences between a treatment and PBS control at each time point. AUCs of fed glucose profiles were compared using one-way ANOVA followed by *post hoc* Tukey's multiple comparison test (n=6). For evaluating AUC of IPGTT

(n=5), treatment and PBS were compared using an unpaired parametric two-tailed t test. Both direct and competitive anti-PEG ELISAs (n=3) were analyzed using two-way ANOVA, followed by *post hoc* Dunnett's multiple comparison test to evaluate individual differences between exendin-C-POEGMA and the other groups for each plasma sample (direct) or antigen concentration (competitive). A test was considered significant if the P value was less than 0.05. Statistical analyses were performed using Prism 6 (GraphPad software Inc.).

Supplementary Material

Refer to Web version on PubMed Central for supplementary material.

Acknowledgments

The authors thank Dr. David M. Gooden at the Duke Small Molecule Synthesis Facility for synthesis of AEBMP, Dr. Erik J. Soderblom at the Duke Proteomics Facility for conducting LC/MS-MS, Dr. George Dubay at the Duke Chemistry Mass Spectrometry Facility for LC/ESI-MS support, and Dr. Mark N. Feinglos, Professor of medicine at Duke University, for discussion of *in vivo* results. BHK cells expressing GLP-1R was a generous gift of the Drucker group (University of Toronto, Canada). This work was supported by National Institute of Health (R01-DK092665 to A.C.).

References

1. Leader B, Baca QJ, Golan DE. Protein therapeutics: a summary and pharmacological classification. Nat Rev Drug Discov. 2008; 7:21–39. [PubMed: 18097458]
2. Craik DJ, Fairlie DP, Liras S, Price D. The future of peptide-based drugs. Chem Biol Drug Des. 2013; 81:136–147. [PubMed: 23253135]
3. Peters TJ. Serum albumin. Adv Protein Chem. 1985; 37:161–245. [PubMed: 3904348]
4. Awai M, Brown EB. Studies of the metabolism of I-131-labeled human transferrin. J Lab Clin Med. 1963; 61:363–396. [PubMed: 13965691]
5. Banga, AK. Therapeutic Peptides and Proteins - Formulation, Processing, and Delivery Systems. CRC Press; 2015.
6. Caliceti P, Veronese FM. Pharmacokinetic and biodistribution properties of poly(ethylene glycol)-protein conjugates. Adv Drug Deliv Rev. 2003; 55:1261–1277. [PubMed: 14499706]
7. Malik DK, Baboota S, Ahuja A, Hasan S, Ali J. Recent advances in protein and peptide drug delivery systems. Curr Drug Deliv. 2007; 2:141–151.
8. Werle M, Bernkop-Schnurch A. Strategies to improve plasma half life time of peptide and protein drugs. Amino Acids. 2006; 30:351–367. [PubMed: 16622600]
9. Alconcel SNS, Baas AS, Maynard HD. FDA-approved poly(ethylene glycol)–protein conjugate drugs. Polym Chem. 2011; 2:1442–1448.
10. Nucci ML, Shorr RG, Abuchowski A. The therapeutic value of poly(ethylene glycol)-modified proteins. Adv Drug Deliv Rev. 1991; 6:133–151.
11. Youn YS, Na DH, Lee KC. High-yield production of biologically active mono-PEGylated salmon calcitonin by site-specific PEGylation. J Control Release. 2007; 117:371–379. [PubMed: 17207880]
12. Gauthier MA, Klok H. Peptide/protein–polymer conjugates: synthetic strategies and design concepts. Chem Commun. 2008:2591–2611.
13. Qi Y, Chilkoti A. Growing polymers from peptides and proteins: a biomedical perspective. Polym Chem. 2014; 5:266–276.
14. Gaberc-Porekar V, Zore I, Podobnik B, Menart V. Obstacles and pitfalls in the PEGylation of therapeutic proteins. Curr Opin Drug Discov Devel. 2008; 11:242–250.
15. Veronese FM. Peptide and protein PEGylation: a review of problems and solutions. Biomaterials. 2001; 22:405–417. [PubMed: 11214751]

16. Ganson NJ, Kelly SJ, Scarlett E, Sundy JS, Hershfield MS. Control of hyperuricemia in subjects with refractory gout, and induction of antibody against poly(ethylene glycol) (PEG), in a phase I trial of subcutaneous PEGylated urate oxidase. Arthritis Res Ther. 2006; 8:R12–R22. [PubMed: 16356199]
17. Hershfield MS, et al. Induced and pre-existing anti-polyethylene glycol antibody in a trial of every 3-week dosing of pegloticase for refractory gout, including in organ transplant recipients. Arthritis Res Ther. 2014; 16:R63. [PubMed: 24602182]
18. Armstrong JK, et al. Antibody against poly(ethylene glycol) adversely affects PEG-asparaginase therapy in acute lymphoblastic leukemia patients. Cancer. 2007; 110:103–111. [PubMed: 17516438]
19. Richter AW, Akerblom E. Polyethylene glycol reactive antibodies in man: titer distribution in allergic patients treated with monomethoxy polyethylene glycol modified allergens or placebo, and in healthy blood donors. Int Arch Allergy Appl Immunol. 1984; 74:36–39. [PubMed: 6706424]
20. Garay RP, El-Gewely R, Armstrong JK, Garratty G, Richette P. Antibodies against polyethylene glycol in healthy subjects and in patients treated with PEG-conjugated agents. Expert Opinion Drug Deliv. 2012; 9:1319–1323.
21. Ganson NJ, et al. Pre-existing anti-PEG antibody linked to first-exposure allergic reactions to Pegnivacogin, a PEGylated RNA aptamer. J Allergy Clin Immunology. 2016; 137:1610–1613. [PubMed: 26688515]
22. Qi Y, Amiram M, Gao W, McCafferty DG, Chilkoti A. Sortase-catalyzed initiator attachment enables high yield growth of a stealth polymer from the C terminus of a protein. Macromol Rapid Commun. 2013; 34:1256–1260. [PubMed: 23836349]
23. Matyjaszewski K, Tsarevsky NV. Macromolecular engineering by atom transfer radical polymerization. J Am Chem Soc. 2014; 136:6513–6533. [PubMed: 24758377]
24. Matyjaszewski K, Xia J. Atom transfer radical polymerization. Chem Rev. 2001; 101:2921–2990. [PubMed: 11749397]
25. Bontempo D, Maynard HD. Streptavidin as a macroinitiator for polymerization: in situ protein-polymer conjugate formation. J Am Chem Soc. 2005; 127:6508–6509. [PubMed: 15869252]
26. Gao W, et al. In situ growth of a stoichiometric PEG-like conjugate at a protein's N-terminus with significantly improved pharmacokinetics. Proc Natl Acad Sci. 2009:15231–15236. [PubMed: 19706892]
27. Gao W, Liu W, Christensen T, Zalutsky MR, Chilkoti A. In situ growth of a PEG-like polymer from the C terminus of an intein fusion protein improves pharmacokinetics and tumor accumulation. Proc Natl Acad Sci. 2010; 107:16432–16437. [PubMed: 20810920]
28. Peeler JC, et al. Genetically encoded initiator for polymer growth from proteins. J Am Chem Soc. 2010; 132:13575–13577. [PubMed: 20839808]
29. Lele BS, Murata H, Matyjaszewski K, Russell AJ. Synthesis of uniform protein-polymer conjugates. Biomacromolecules. 2005; 6:3380–3387. [PubMed: 16283769]
30. Ryan SM, et al. PK/PD modelling of comb-shaped PEGylated salmon calcitonin conjugates of differing molecular weights. J Control Release. 2011; 149:126–132. [PubMed: 20946924]
31. Magnusson JP, Bersani S, Salmaso S, Alexander C, Caliceti P. In situ growth of side-chain PEG polymers from functionalized human growth hormone-a new technique for preparation of enhanced protein-polymer conjugates. Bioconjugate Chem. 2010; 21:671–678.
32. Lovshin JA, Drucker DJ. Incretin-based therapies for type 2 diabetes mellitus. Nat Rev Endocrinol. 2009; 5:262–269. [PubMed: 19444259]
33. Boekhorst J, de Been MW, Kleerebezem M, Siezen RJ. Genome-wide detection and analysis of cell wall-bound proteins with LPxTG-like sorting motifs. J Bacteriol. 2005; 187:4928–4934. [PubMed: 15995208]
34. Meyer DE, Chilkoti A. Purification of recombinant proteins by fusion with thermally-responsive polypeptide. Nat Biotechnol. 1999; 14:1112–1115.
35. Mao H, Hart SA, Schink A, Pollok BA. Sortase-mediated protein ligation: a new method for protein engineering. J Am Chem Soc. 2004:126.

36. Jakubowski W, Matyjaszewski K. Activators regenerated by electron transfer for atom-transfer radical polymerization of (meth)acrylates and related block copolymers. Angew Chem Int Ed. 2006; 45:4482–4486.
37. Goke R, et al. Exendin-4 is a high potency agonis and truncated exendin-(9-39)-amide an antagonist at the glucagon-like peptide 1-(7-36)-amide receptor of insulin-secreting b-cells. J Biol Chem. 1993; 268:19650–19655. [PubMed: 8396143]
38. Winzell MS, Ahren B. The high-fat diet-fed mouse: a model for studying mechanisms and treatment of impaired glucose tolerance and type 2 diabetes. Diabetes. 2004; 53:S215–S219. [PubMed: 15561913]
39. Surwit RS, Kuhn CM, Cochrane C, McCubbin JA, Feinglos MN. Diet-induced type II diabetes in C57BL/6J mice. Diabetes. 1988; 37:1163–1167. [PubMed: 3044882]
40. Mack CM, et al. Antiobesity action of peripheral exenatide (exendin-4) in rodents: effects on food intake, body weight, metabolic status and side-effect measures. Int J Obes. 2006; 30:1332–1340.
41. Kanoski SE, Rupperecht LW, Fortin SM, De Jonghe BC, Hayes MR. The role of nausea in food intake and body weight suppression by peripheral GLP-1 receptor agonists, exendin-4 and liraglutide. Neuropharmacology. 2012; 62:1916–1927. [PubMed: 22227019]
42. Richter AW, Akerblom E. Antibodies against polyethylene glycol produced in animals by immunization with monomethoxy polyethylene glycol modified proteins. Int Arch Allergy Appl Immunol. 1983; 70:124–131. [PubMed: 6401699]
43. Tsarevsky NV, Pintauer T, Matyjaszewski K. Deactivation efficiency and degree of control over polymerization in ATRP in protic solvents. Macromolecules. 2004; 37:9768–9778.
44. Averick S, et al. Protein-polymer hybrids: conducting ARGET ATRP from a genetically encoded cleavable ATRP initiator. Eur Polym J. 2013; 49:2919–2924.
45. Bellucci JJ, Bhattacharyya J, Chilkoti A. A noncanonical function of sortase enables site-specific conjugation of small molecules to lysine residues in proteins. Angew Chem Int Ed. 2015; 54:441–445.
46. Amiram M, Luginbuhl KM, Li X, Feinglos MN, Chilkoti A. Injectable protease-operated depots of glucagon-like peptide-1 provide extended and tunable glucose control. Proc Natl Acad Sci. 2013; 110:2792–2797. [PubMed: 23359691]
47. Schellenberger V, et al. A recombinant polypeptide extends the in vivo half-life of peptides and proteins in a tunable manner. Nat Biotechnol. 2009; 27:1186–1188. [PubMed: 19915550]
48. Liao YD, Jeng JC, Wang CF, Wang SC, Chang ST. Removal of N-terminal methionine from recombinant proteins by engineered E. coli methionine aminopeptidase. Prot Sci. 2004; 13:1802–1810.
49. McDaniel JR, Mackay JA, Quiroz FG, Chilkoti A. Recursive directional ligation by plasmid reconstruction allows rapid and seamless cloning of oligomeric genes. Biomacromolecules. 2010; 11:944–952. [PubMed: 20184309]
50. Ilangovan U, Ton-That H, Iwahara J, Schneewind I, Clubb RT. Structure of sortase, the transpeptidase that anchors proteins to the cell wall of Staphylococcus aureus. Proc Natl Acad Sci. 2001; 98:6056–6061. [PubMed: 11371637]
51. Drucker DJ, Nauck MA. The incretin system: glucagon-like peptide-1 receptor agonists and dipeptidyl peptidase-4 inhibitors in type 2 diabetes. Lancet. 2006; 368:1696–1705. [PubMed: 17098089]
52. Baggio LL, Huang QL, Brown TJ, Drucker DJ. A recombinant human glucagon-like peptide (GLP)-1- albumin protein (Albugon) mimics peptidergic activation of GLP-1 receptor-dependent pathways coupled with satiety, gastrointestinal motility, and glucose homeostasis. Diabetes. 2004; 53:2492–2500. [PubMed: 15331566]
53. Goutelle S, et al. The Hill equation: a review of its capabilities in pharmacological modelling. Fundam Clin Pharmacol. 2008; 22:633–648. [PubMed: 19049668]
54. Qi, Y., et al. Dataset for A brush-polymer conjugate of exendin-4 reduces blood glucose for up to five days and eliminates poly(ethylene glycol) antigenicity. figshare. 2016. http://dx.doi.org/10.6084/m9.figshare.3976761

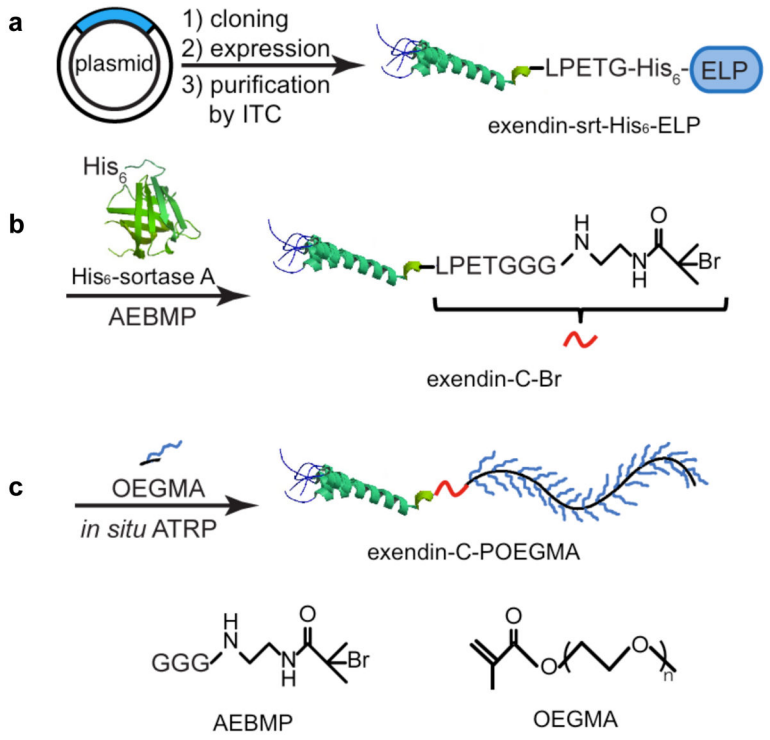

Fig. 1.

Synthetic scheme of exendin-C-POEGMA. **a**) Recombinant expression of the sortase A substrate, exendin-srt-His_6-ELP, and purification by ITC [34]. **b**) Sortase-catalyzed site-specific attachment of the ATRP initiator AEBMP to the C-terminus of exendin to generate exendin-C-Br. **c**) *In situ* ATRP of OEGMA from exendin-C-Br yielding exendin-C-POEGMA. ITC: inverse transition cycling, ELP: elastin-like polypeptide, srt: sortase A recognition sequence "LPETG", AEBMP: N-(2-(2-(2-(2-aminoacetamido)acetamido)acetamido) ethyl)-2-bromo-2-methylpropanamide.

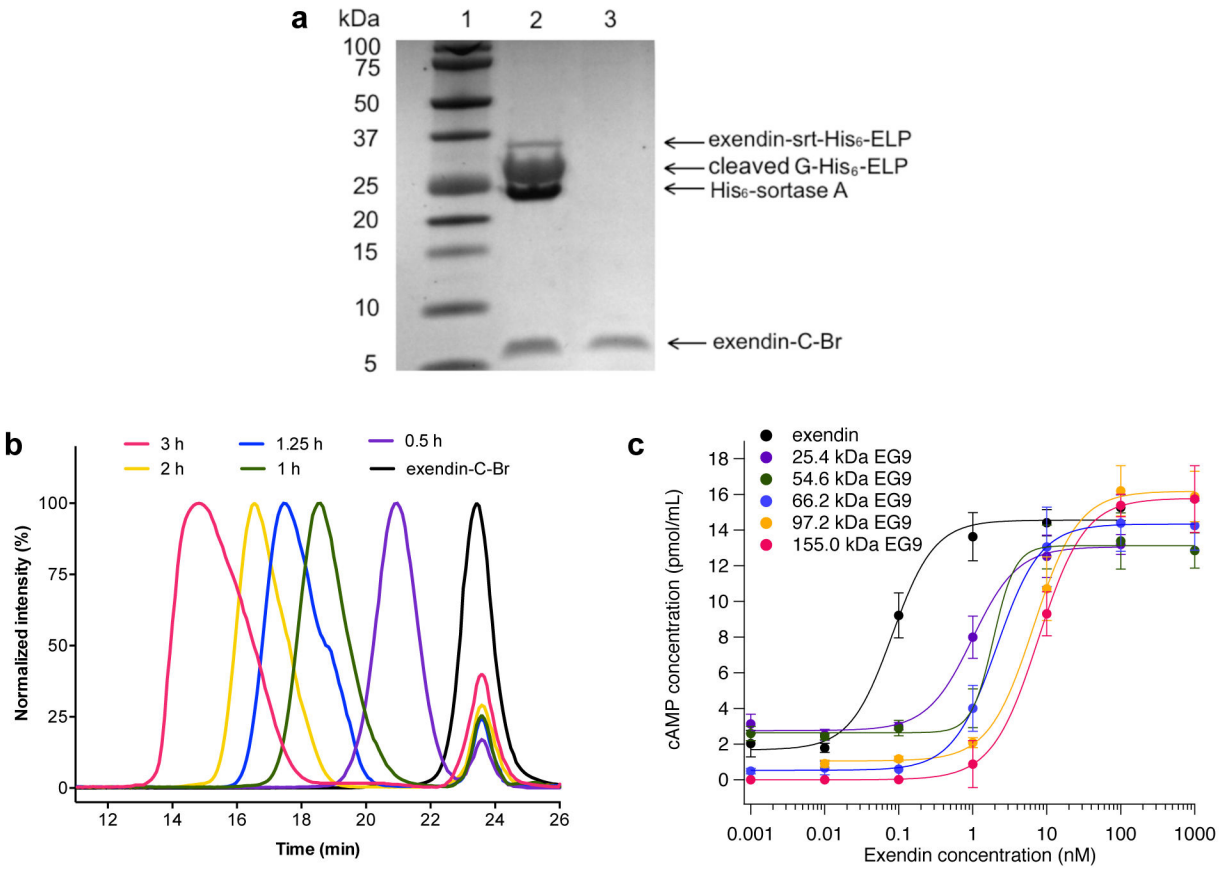

Fig. 2.

Characterization of exendin-C-Br macroinitiator and EG9 exendin-C-POEGMA conjugates. **a**) Coomassie-stained SDS-PAGE analysis of initiator attachment on exendin by sortase A. Lane 1: MW marker, lane 2: sortase reaction mixture after 18 h of reaction, lane 3: purified exendin-C-Br macroinitiator. **b**) SEC traces of ATRP reaction mixtures of grafting EG9 POEGMA from exendin-C-Br carried out for 0.5 h, 1 h, 1.25 h, 2 h and 3 h, detected by UV-vis absorbance at 280 nm. **c**) Cyclic adenosine monophosphate (cAMP) response of native exendin and EG9 exendin-C-POEGMA conjugates with M_ns of 25.4 kDa, 54.6 kDa, 66.2 kDa, 97.2 kDa and 155.0 kDa in baby hamster kidney (BHK) cells expressing the GLP-1R. Results are plotted as mean ± standard error of the mean (SEM), n=3. Half-maximal effective concentration (EC_{50}) values are summarized in Table 1.

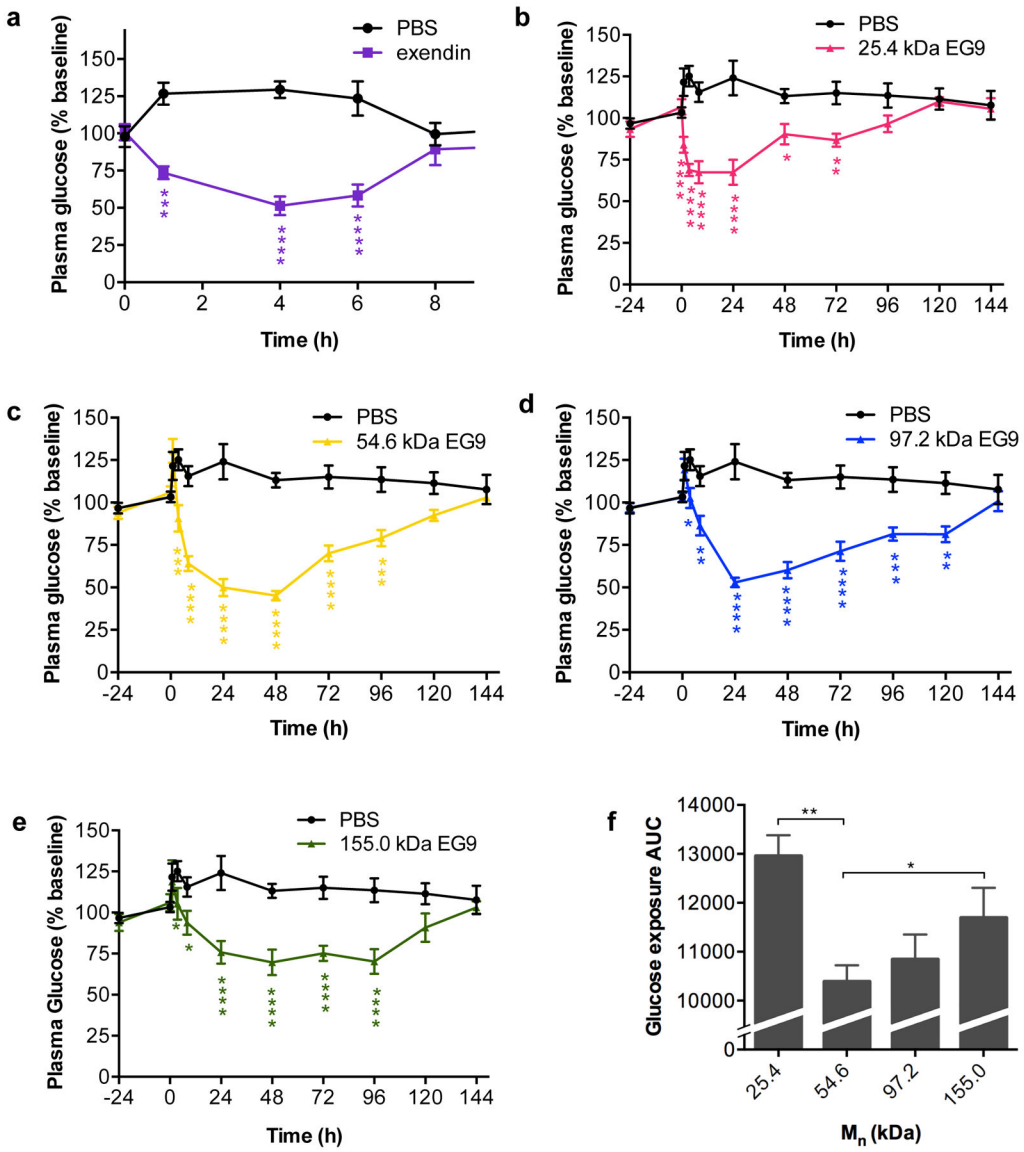

Fig. 3.

Assessment of MW-dependent *in vivo* efficacy of EG9 exendin-C-POEGMA conjugates. Blood glucose levels in fed mice were measured before and after a single s.c. injection of **a**) unmodified exendin, or **b-e**) 25.4 kDa, 54.6 kDa, 97.2 kDa, and 155.0 kDa EG9 exendin-C-POEGMA conjugates, compared to PBS control. The peptide and conjugates were administered at 25 nmol/kg and PBS was injected at equivalent volume at t = 0 h. Blood glucose levels were normalized to the average glucose levels measured 24 h and immediately before injection. Data were analyzed by repeated measures two-way analysis of variance (ANOVA), followed by *post hoc* Dunnett's multiple comparison test. **f**) Area under the curve (AUC) of blood glucose profiles (0 h to 144 h, with respect to 0% baseline) as a function of conjugate M_n. AUCs were compared using one-way ANOVA followed by *post hoc* Tukey's multiple comparison test. In all panels, results are plotted as mean ± SEM, n=6, $*P < 0.05$, $**P < 0.01$, $***P < 0.001$ and $****P < 0.0001$.

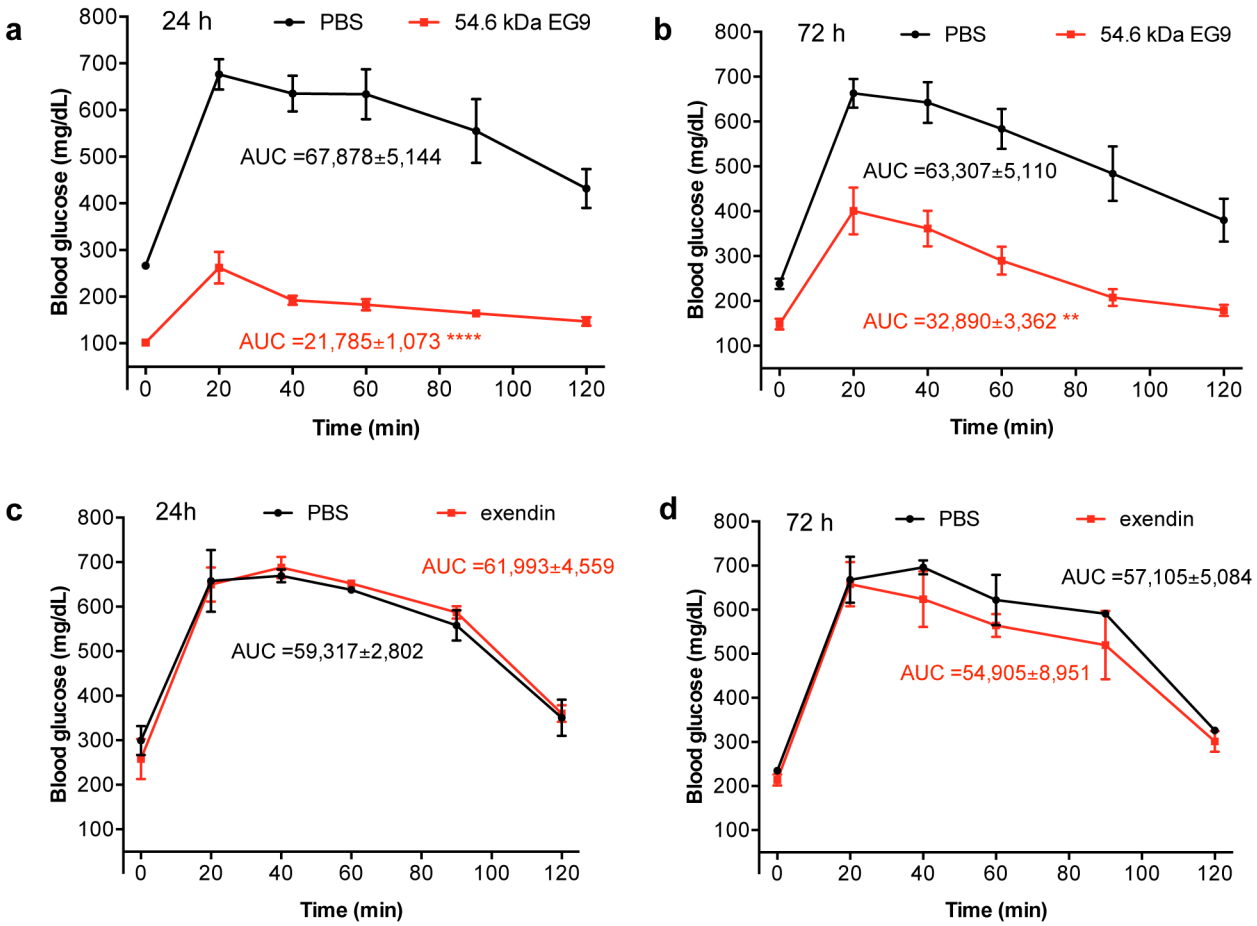

Fig. 4.

Intraperitoneal glucose tolerance test (IPGTT) of an EG9 exendin-POEGMA in mice. Mouse blood glucose levels measured in an IPGTT performed at 24 h and 72 h after a single s.c. injection of **a** and **b**) the 54.6 kDa EG9 exendin-POEGMA conjugate or **c** and **d**) unmodified exendin at 25 nmol/kg, compared to PBS of equivalent volume. Mice were fasted for 6 h prior to glucose challenge by an intraperotoneal (i.p.) injection of 1.5 g/kg of glucose. Results are plotted as mean ± SEM, n=5 in panels a and b, n=3 in panels c and d. AUCs of treatment and PBS were compared using an unpaired parametric two-tailed t test (** $P < 0.01$, and **** $P < 0.0001$). Exendin was not significant at either time point.

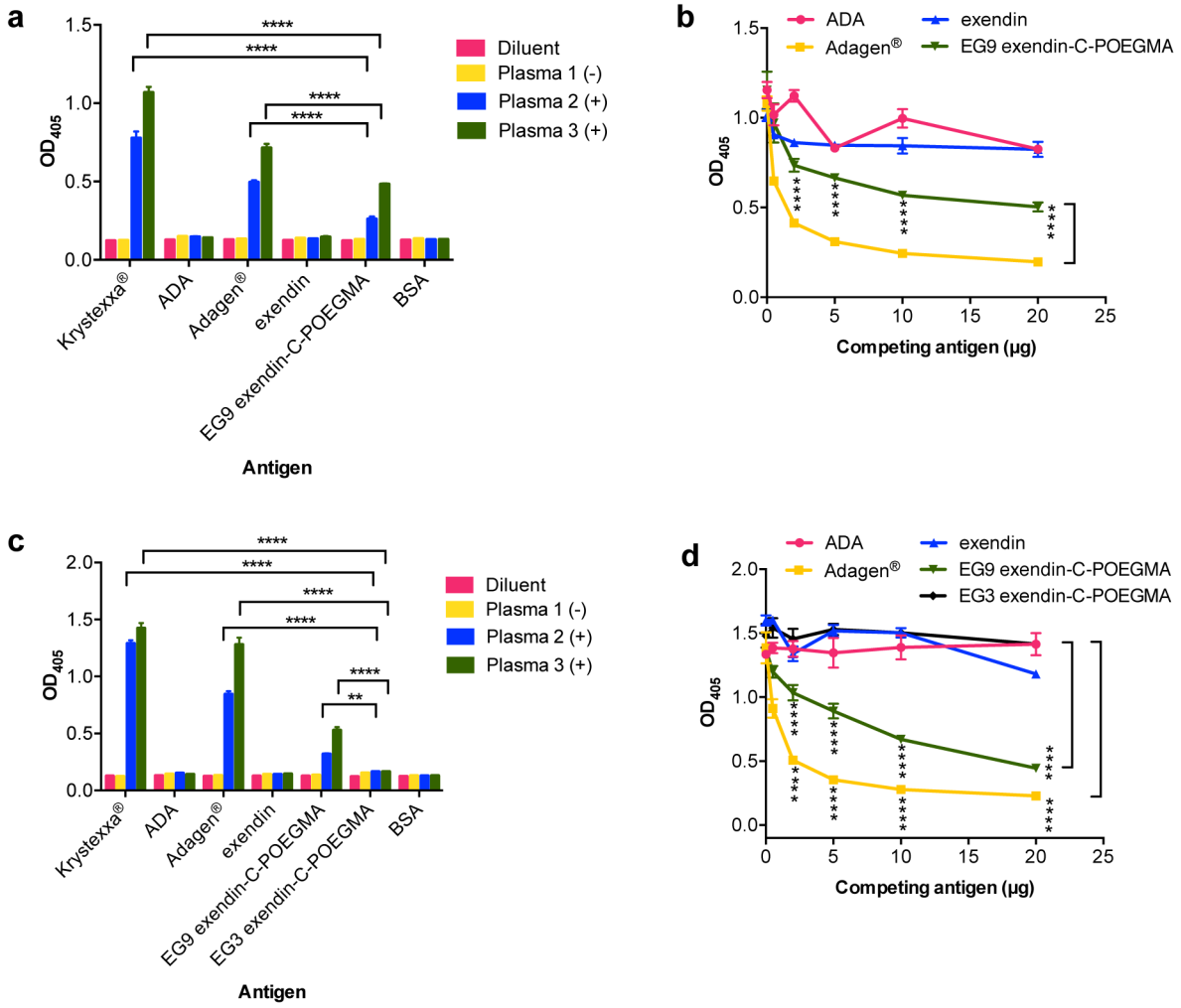

Fig. 5.

Assessment of reactivity of exendin-C-POEGMA conjugates toward anti-PEG antibodies in patient plasma samples. **a**) Direct ELISA probing 54.6 kDa EG9 exendin-C-POEGMA conjugate, native exendin, adenosine deaminase (ADA), bovine serum albumin (BSA), Krystexxa® (PEG-uricase) and Adagen® (PEG-ADA) with diluent (1% BSA in PBS), an anti-PEG negative patient plasma sample, or one of two anti-PEG positive plasma samples. **b**) Competitive ELISA, where various amounts of exendin, 54.6 kDa EG9 exendin-C-POEMGA, ADA and Adagen® were allowed to compete with Krystexxa® for binding with anti-PEG antibodies in a positive plasma sample. **c** and **d**) Direct and competitive assays described in panels a and b performed with a 55.6 kDa EG3 exendin-C-POEGMA conjugate. In all assays, the same unmodified peptide/protein content or similar PEG/OEG content in the case of polymer-modified samples per well were compared. See Methods section for details. Results are plotted as mean ± SEM, n=3 in panels a and b, n=5 in panels c and d. Data were analyzed by two-way ANOVA, followed by *post hoc* Dunnett's multiple comparison test (**$P < 0.01$, and ****$P < 0.0001$).

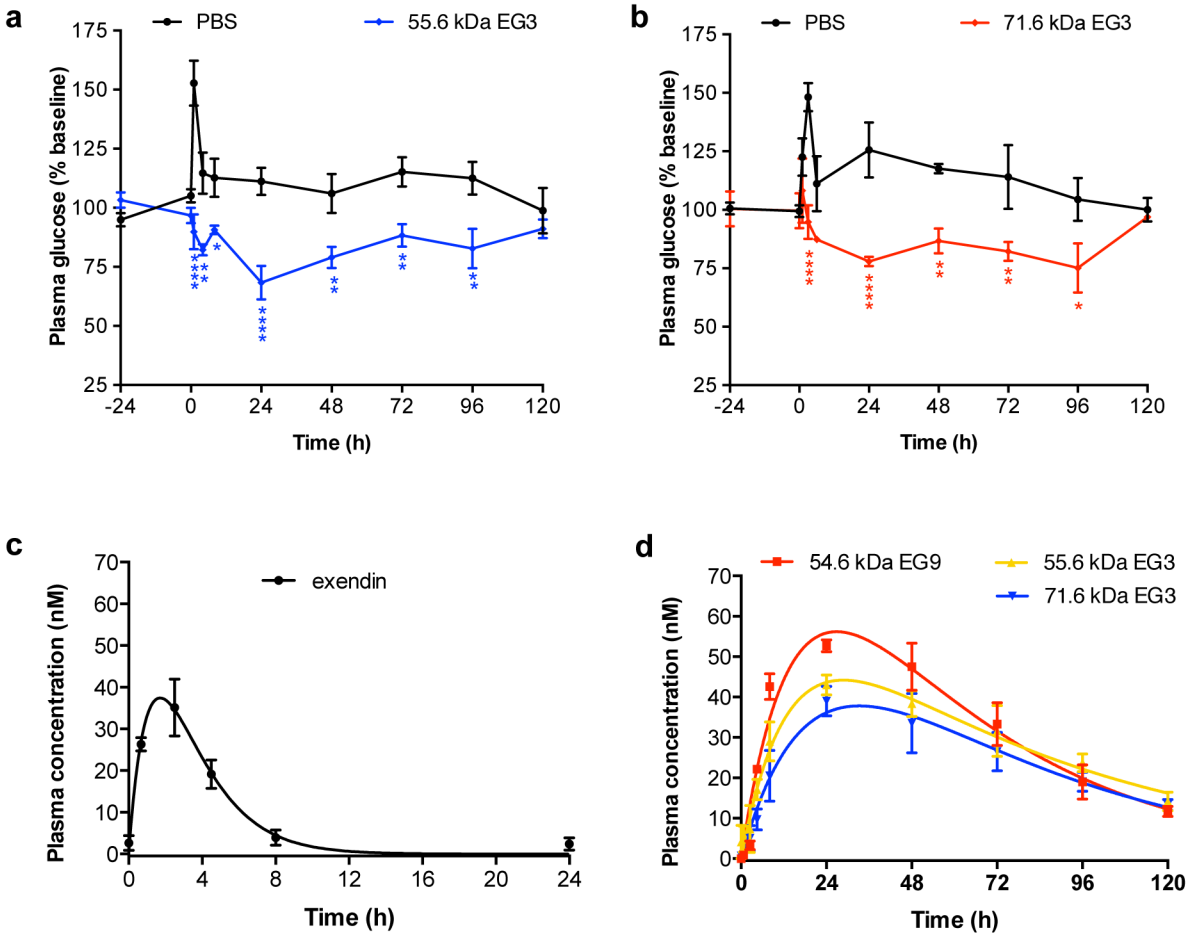

Fig. 6.

Assessment of *in vivo* efficacy and pharmacokinetics of exendin-C-POEGMA conjugates. Blood glucose levels in fed mice measured before and after a single s.c. injection of **a**) 55.6 kDa and **b**) 71.6 kDa EG3 exendin-C-POEGMA conjugates at 25 nmol/kg or PBS at equivalent volume administered at t = 0 h. Blood glucose levels were normalized to the average glucose levels measured 24 h and immediately before injection. Data were analyzed by repeated measures two-way ANOVA, followed by *post hoc* Dunnett's multiple comparison test (n=5, $*P < 0.05$, $**P < 0.01$, and $****P < 0.0001$). **c**) Exendin and **d**) exendin-C-POEGMA conjugates (54.6 kDa EG9, 55.6 kDa EG3 and 71.6 kDa EG3) were fluorescently labeled with Alexa Fluor® 488 and injected into mice (n=3) s.c. at 75 nmol/kg (45 nmol/kg fluorophore). Blood samples were collected via tail vein at various time points for fluorescence quantification. Data were analyzed using a non-compartmental fit (solid lines) to derive the pharmacokinetic parameters shown in Table 2. Results in all panels are plotted as mean ± SEM.

Table 1

Physical properties and biological activity of exendin and exendin-C-POEGMA conjugates.

Species	Reaction time (h)	M_w (Da)	M_n (Da)	$Đ$ (M_w/M_n)	R_h (nm)	EC_{50} (nM)
exendin	--	--	4,186.6[a]	1.00[b]	2.2 ± 0.1	0.08 ± 0.01
EG9	0.5	26,400	25,400	1.04	4.5 ± 0.4	0.84 ± 0.09
EG9	1	56,800	54,600	1.04	5.6 ± 0.5	1.91 ± 0.35
EG9	1.25	72,200	66,200	1.09	5.9 ± 0.5	2.10 ± 0.08
EG9	2	100,000	97,200	1.03	6.8 ± 0.7	6.67 ± 0.21
EG9	3	178,000	155,000	1.15	7.6 ± 0.5	7.69 ± 0.04
EG3	3	27,400	26,300	1.04	3.8 ± 0.4	3.29 ± 0.27
EG3	5.5	60,600	55,600	1.09	4.8 ± 0.5	4.17 ± 0.13
EG3	8	82,700	71,600	1.16	5.4 ± 0.6	5.11 ± 0.23

MWs and *Đ*s were determined by size exclusion chromatography multi-angle light scattering (SEC-MALS). R_hs were measured by dynamic light scattering (DLS). EC_{50} values of EG9 and EG3 conjugates were derived from cAMP response curves in Fig. 2c and Supplementary Fig. S7, respectively. R_h and EC_{50} values are reported as mean ± SEM, n=10 for R_h and n=3 for EC_{50}. M_w: weight-average MW, M_n: number-average MW, *Đ*: dispersity, R_h: hydrodynamic radius, EC_{50}: half-maximal effective concentration.

[a]Calculated from amino acid sequence.

[b]Default value due to unimolecular nature of the peptide.

Table 2

Pharmacokinetic parameters of exendin and exendin-C-POEGMA conjugates injected s.c. derived from data analyzed with a non-compartmental fit in Figs. 6c and d.

	$t_{1/2\ a}$ (h)	$t_{1/2\ el}$ (h)	C_{max} (nM)[a]	t_{max} (nM)[a]	AUC (h*nM)[b]
exendin	0.7±0.1	1.7±0.2	37.1±3.8	1.78±0.1	217.5±36.5
54.6 kDa EG9	6.2±0.5	42.4±2.9	56.4±3.9	20.1±0.4	4,795.5±440.7
55.6 kDa EG3	7.6±0.7	61.2±5.0	44.0±2.7	28.5±2.3	4,775.0±482.9
71.6 kDa EG3	9.0±1.7	61.5±3.2	37.7±5.0	32.4±3.9	4,411.2±499.6

Values are reported as mean ± SEM. $t_{1/2\ a}$: absorption half-life, $t_{1/2\ el}$: elimination half-life, C_{max}: maximum plasma concentration, t_{max}: time to attain C_{max}.

[a] Derived from curve fitting.

[b] Calculated from t = 0 to ∞ from curve fitting.